

# X-f choice reconstruction of dynamic undersampled MR data applied to DCE-MRA

S. Malik<sup>1</sup>, S. Schmitz<sup>1</sup>, D. O'Regan<sup>1</sup>, J. Hajnal<sup>1</sup>

<sup>1</sup>Robert Steiner MRI Unit, Imaging Sciences Department, MRC Clinical Sciences Centre, Hammersmith Hospital, Imperial College London, London, England, United Kingdom

**Introduction** Undersampling in the 'k-t' domain is increasingly used for dynamic acquisitions where regions of the image requiring a high frame rate do not fill the whole field of view. Undersampling produces aliasing in the conjugate 'x-f' (space and temporal frequency) domain which reconstruction schemes must resolve. Typically there is a trade off between alias suppression, SNR and spatiotemporal blurring depending on how this problem is solved. For example k-t BLAST [1] uses a low resolution training scan to estimate the signal distribution in x-f space and then constructs a filter to remove aliases. The x-f choice reconstruction [2] scheme avoids temporal blurring seen in other methods by taking advantage of the observation that the signal at each point in the aliased space generally has contributions from only a subset of the total that are possible. Presented is a x-f choice reconstruction in which information about signal content is 'learned' from the aliased data itself using a clustering approach, meaning that no training scan is required, and full use is made of array coil data. The method is applied here to dynamic contrast enhanced MRA (DCE-MRA).

**Methods: reconstruction scheme** The signal in the aliased x-f domain is the complex sum of the signal from contributing points in the fully sampled (unknown) x-f space; lattice undersampling results in aliases from a discrete set of points. With multiple receiver coils, this aliased x-f space is viewed independently by each coil. In this case the signal can be described as  $s_i = C_{ij} \rho_j$  where  $s_i$  is the aliased signal viewed by the  $i^{\text{th}}$  receiver coil,  $C_{ij}$  is the sensitivity of the  $i^{\text{th}}$  coil at the  $j^{\text{th}}$  aliased point and  $\rho_j$  is the unknown signal from that point in x-f space. For a problem with  $n$ -fold acceleration and  $\chi$  coil views, reconstruction requires inversion of  $\mathbf{C}$  which may be badly conditioned or under determined ( $n > \chi$ ). Fig 1 shows a typical aliased x-f space and a single spectrum taken from it ( $n=5$ ). The number of contributing aliases at each point in this spectrum is less than 5 since not all spatial locations contributing to the aliased signal have strong dynamic content. To characterise this property the separate aliases are fitted with 'envelope functions' (coloured dotted lines in fig 1) designed to estimate signal contribution from each alias across the full temporal bandwidth.

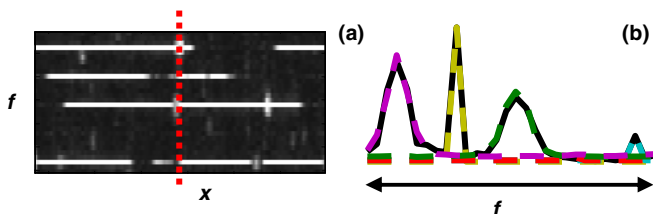


**Fig.1** a) Five fold aliased x-f space from phantom experiment. b) Spectrum from dotted line marked on a (black line). The coloured dotted lines are envelope functions fitted to the aliased spectrum

For each point in the 4-dim x-f space the g-factor noise amplification cost of reconstructing problems of different sizes is calculated. Removing columns from  $\mathbf{C}$  and setting corresponding elements of  $\rho$  to zero reduces the problem and the fitted envelope functions are used to estimate the error caused by doing this. An 'optimal' problem size for the reconstruction for each voxel is inferred such that the estimated error is less than the noise level. This optimal size reflects the true amount of aliasing at this point. Under determined problems are solved by first reducing the problem until it is tractable.

Envelope functions are generated from the aliased data itself. The lowest frequency Fourier components of each f-spectrum in the aliased space have a characteristic shape which can be used to indicate the temporal behaviour

of that voxel. K-means clustering is used to classify each voxel, using these portions of the f-spectrum as a feature vector. Groups corresponding to highly dynamic voxels are identified. Knowledge of the undersample pattern is then used to exclude dynamic voxels that alias onto others with dynamic content. The remaining voxels are deemed to have correct information across the whole temporal bandwidth and their spectra are used to generate the envelope functions used in the rest of the reconstruction. Since redundancy in dynamic data is exploited in this step, no training scan is required.

**Data acquisition** Dynamic undersampling has been implemented on a Philips 3T Intera system. A standard T1FFE angiographic sequence (TR/TE/FA = 2.6ms/0.89ms/13°) was used in conjunction with undersampling. A six element phased array coil was used for all studies. Following tests on power injector driven water phantoms, the method was validated by post acquisition undersampling of a fully sampled DCE-MRA obtained from a healthy volunteer using reduced coverage to give adequate temporal resolution. Three *in vivo* undersampled studies of the legs at the level of the knees using 5-fold undersampling have been performed, including one patient. Typically 7n frames were acquired over a period of approximately 200s while contrast was administered using a power injector.

**Results** The validation study showed max. errors were < 5% at peak signal up to  $n = 10$  but SNR falls off and ultimately limits the method. Notably no temporal blurring was observed; errors primarily appear to come from noise amplification, part of which is inherent for undersampling techniques. All images reconstructed from undersampled acquisitions have good suppression of aliases without obvious spatiotemporal blurring. Three time frames from a scan of a patient with peripheral atherosclerotic disease are given in fig.2. Spatial resolution was  $1.56 \times 1.56 \times 3 \text{ mm}^3$  with temporal resolution increased from 24s to 4.7s by undersampling. The peak arterial frame (fig 2b) compares well with a DSA image (fig 2d) taken on the same day, and the high time resolution shows delayed filling in one leg (fig 2a) which would have otherwise been unobservable.



**Fig. 2** Selected single time points from patient study of the legs, all shown in coronal maximum intensity projection using inverted greyscale. Times after injection are 23s, 32s and 70s for a,b and c respectively. d) X-ray DSA image of the same patient on the same day.

**Conclusions** The properties of x-f space are such that aliased signals are generally dominated by only a subset of the possible contributors. X-f choice estimates which these are from model spectral shapes 'learned' from the aliased data itself using a clustering technique and adjusts the reconstruction to take this into account. Noise amplification from use of parallel imaging techniques is regulated with this step since data is reconstructed using modest problem sizes even where the actual undersampling is much higher. No training scan is required. By using full temporal bandwidth envelope functions to estimate the signal content, low pass filtering is avoided meaning that the temporal blurring seen with filter based reconstructions is not seen with this method. Although the formulation includes multiple receive coils, it is also possible to use x-f choice on single coil data by reducing the problem to a single alias in all locations. DCE-MRA has favourable properties for k-t undersampling, i.e. very sparse dynamic change; however we expect that the x-f choice method may be generally applied to k-t undersampled data.

**References** 1. Tsao J et al., Magn Reson Med. 2003 Nov;50(5):1031-42. 2. Malik SJ et al., Proceedings of ISMRM 2005

**Acknowledgement** We thank Philips Medical systems for research grant support